Relativistic DFT calculations for neutral and singly charged Au_2

Aqeel Mohsin Ali*

Polymer Research Center, University of Basrah, Basrah, Iraq

*Corresponding Author: aqeel.mohsin@uobasrah.edu.iq

Received 29 Aug. 2024, Accepted 13 June. 2025, published 30 Dec. 2025.

DOI: 10.52113/2/12.02.2025/14-20

Abstract: The study explores the use of relativistic Density Functional Theory (DFT) using the Gaussian09 package to analyze the geometry optimization of gold diatoms in various ionic states. The optimization is performed at multiple theoretical levels, including B3LYP, cam-B3LYP, PBEPBE, HSE1PBE, and HSE2PBE, utilizing SDD and LaNL2MB basis sets. An investigation has been conducted on all structures to analyze their ionization potential, electron affinity, electrostatic potential contours, infrared spectra, molecular orbitals, energy gap, and electronic excitation. The ionization potential and electron affinity of all structures exhibit strong agreement with the experimental results. The molecular orbitals of bonding and anti-bonding nature undergo significant changes based on the ionic state. The electron charge density in a gold diatom determines the electrostatic potential contours, vibration frequency, and electronic excitation.

***Keywords*:** Relativistic DFT, Gold diatom, Ionization potential, Electron affinity, Molecular orbitals, optical spectrum.

1. Introduction

Gold clusters are now generating attention as the fundamental components of innovative nanostructured materials and electronics [1]. Over the last twenty years, scientists have conducted research on the composition of gold clusters using both experimental and theoretical methods [2]. Experimental findings indicate that gold nanoclusters with diameters ranging from 1 to 2 nm lack a crystalline structure and are thus considered amorphous [3]. The argument is further supported by theoretical findings derived from empirical molecular dynamics simulations or first principles computations. Over the last 30 years, there has been much research on the composition and electrical characteristics of gold clusters using several theoretical approaches. Hakkinen and Landman examined the neutral particles and anions of Au_{2-10} clusters using the generalized gradient approximation (GGA) [4]. Gronbech and Andreoni conducted a comparison between Au_2 and Au_5 using the spin-polarized Becke-Lee-Yang-Parr (BLYP) functional [5]. Bravo-Pérez et al. examined tiny gold clusters consisting of up to six atoms using the ab initio Hartree-Fock (HF) and post-HF methods [6]. Kuang et al. conducted scalar relativistic all-electron density-functional theory (DFT) calculations on various small gold clusters and study the effect of electron pairing [7]. Wang and Zhou investigated tiny structures in Au_n (n=

1,8,13) clusters on TiO_2 nanotubes by using pseudopotential DFT simulations within the GGA-PBE method [8]. Furthermore, there are further studies about the global minimum structures of medium-sized gold clusters using empirical potentials.

Although significant advancements have been made, there are still unresolved inquiries about gold clusters. There is currently no experimental data on the architectures of Au_n clusters with more than n=2 atoms [9]. Therefore, a precise first-principles computation is crucial for comprehending the structural and electrical characteristics of these clusters. Prior ab initio computations on gold clusters were constrained by assumed symmetrical limitations. A comprehensive exploration of the cluster potential energy surface without limitations is required. This study involves the production of gold diatom with three ionic states using DFT simulations. The study examines the comparative stability, electronic density of states, HOMO-LUMO gap (the energy difference between the highest occupied and lowest empty molecular orbit), ionization potentials, electron affinity, vibration and optical excitation of gold clusters.

2. Methodology

This study involves doing self-consistent-field (SCF) electronic structure calculations on gold clusters using the Gaussian 09 software [10], which is based on density functional theory (DFT). The computations use a relativistic effective core potential (ECP) together with a double numerical basis that include a d-polarization function. The electron density functional is analyzed using the B3LYP, cam-B3LYP, PBEPBE, HSE1PBE and HSE2PBE hybrid functional. Two basis set implemented in this study for relativistic computations, SDD and LanL2MB. The relativistic effects performed by using scalar relativistic core Hamiltonian through Douglass-Kroll-Hess 0th order [11].

3. Results and Discussion

At first, it should to perform the theoretical hybrids functional and the basis sets, through the test of ionization potential and electron affinity of gold atom and diatom, to predict the electronic properties in good agreement with the experimental results. Tables 1 and 2 show the IP and EA of Au atom and Au diatom. For IP computations, all the hybrid functional are predicted it with good agreement with the experimental value [12,13]. The most accurate theoretical methods are cam-B3LYP (long-range-corrected-B3LYP employ the Coulomb-attenuating routine) and HSE1PBE (full Heyd-Scuseria-Ernzerhof functional with PBE hybrid) with both SDD and LanL2MB basis sets. In the another side of EA computations, the hybrid functional performed in good manner with SDD basis set to calculated the EA of Au atom. For Au diatom, the all hybrid functional have converged EA values for both SDD and LanL2MB basis sets.

Table 1: The ionization potential of Au atom and Au_2 diatom

Method	IP (eV)			
	Au		Au_2	
	SDD	LanL2 MB	SDD	LanL2 MB
B3LYP	9.44	9.34	9.27	9.31
CAM-B3LYP	9.26	9.19	9.06	9.10
PBEPBE	9.59	8.87	9.41	9.38
HSE1PBE	9.28	9.29	9.14	9.21
HSE2PBE	9.52	9.48	9.37	9.45
Exp.	9.23		9.5 ± 0.3	

Table 2: The electron affinity of Au atom and Au_2 diatom

Method	EA (eV)			
	Au		Au_2	
	SDD	LanL 2MB	SDD	LanL 2MB
B3LYP	2.22	1.63	1.95	1.99
CAM-B3LYP	2.03	1.47	1.85	1.90
PBEPBE	2.30	1.63	1.97	1.98
HSE1PBE	2.31	1.49	1.85	1.89
HSE2PBE	2.25	1.74	2.06	2.11
Exp.	2.31		1.94	

Here will provide a concise overview of our findings, which are shown in Table 3. The primary motivation for studying this basic diatomic compound is from the relativistic 6s contraction in the gold atom, which leads to a substantial relativistic bond contraction in Au_2. According to the results in tables 1 and 2, the SDD basis set is implemented with all the hybrid functional to predict the bond length (r_e (Å)) and dissociation energy (D_e (eV)) of neutral, positive and negative charged Au_2. Table III presented the computed bond lengths and dissociation energies in compared with the experimental values [14,15]. From the results, it is clear that the PBEPBE functional (PBE pure functional (exchange and correlation)) has the more accurate prediction for both bond lengths and dissociation energies in compare with the experimental results. The data shown in Table 3 indicate that at the PBEPBE/SDD level, the neutral dimer is predicted to has a relativistic value of bond length ≈ 2.55 Å (Exp. = 2.47 Å), the cationic dimer is predicted to has a value of 2.68 Å, and the anionic dimer is predicted to has a value of 2.68 Å (Exp. = 2.58 Å). The relativistic prediction to the dissociation energy is largest for the neutral and lowest for the anion as $Au_2 > Au_2^+ > Au_2^-$. This phenomenon may be easily described using a basic molecular orbital model. The relativistic lowering of the 6s atomic orbital in gold primarily results in the stability of the σ-HOMO and σ*-LUMO in the dimer. Hence, the bond energy's relativistic component is contingent upon the occupancy of these orbitals. Since only the σ-orbital involved in bonding is occupied in Au_2^-, the relativistic effect on bonding is negligible compared to the neutral and cation forms.

Table 3: The bond length and dissociation energy.

Method	**Au_2**		**Au_2^+**		**Au_2^-**	
	r_e (Å)	D_e (eV)	r_e (Å)	D_e(eV)	r_e (Å)	D_e (eV)
B3LYP	2.58	1.86	2.70	2.03	2.72	1.59
CAM-B3LYP	2.55	1.77	2.68	1.97	1.69	1.60
PBEPBE	2.55	2.22	2.65	2.39	2.68	1.88
HSE1PBE	2.55	1.95	2.68	2.09	2.68	1.75
HSE2PBE	2.55	1.95	2.78	2.00	2.83	1.84
Exp.	2.47	2.30	2.63	2.0 ± 0.3	2.58	1.94

Table 4: The HOMO, LUMO and energy gap.

Model	HOMO (eV)	LUMO (eV)	E_g (eV)
Au_2	-6.216	-4.155	2.061
Au_2^+	-12.685	-10.138	2.547
Au_2^-	0.457	2.556	2.099

The surfaces were examined using molecular orbitals (MOs) at the highest occupied molecular orbital (HOMO) and lowest unoccupied molecular orbital (LUMO) electronic states. The optimization process was used to get surface forms. The process of geometry optimization is halted upon the discovery of a stationary point, specifically when the force resultant is equal to zero. The Gaussian 09 software program is used to calculate the Molecular orbitals for Au_2, Au_2^+, and Au_2^-. The terms "High occupied molecular orbital (HOMO)" and "low unoccupied molecular orbital (LUMO)" refer to the electronic states where electrons may be found in an orbital. The energy gap (E_g) is defined as the difference in energy between two electronic states. Table 4 presents the HOMO, LUMO energies, and energy gap (E_g) for Au_2, Au_2^+, and Au_2^-. Figure 1 showed the contour maps of HOMO and LUMO energy orbitals. The two electrons in Au_2 and the single electron in Au_2^+ occupied the σ-bonding orbital, while the single electron at the Au_2^- case occupied the σ-antibonding orbital.

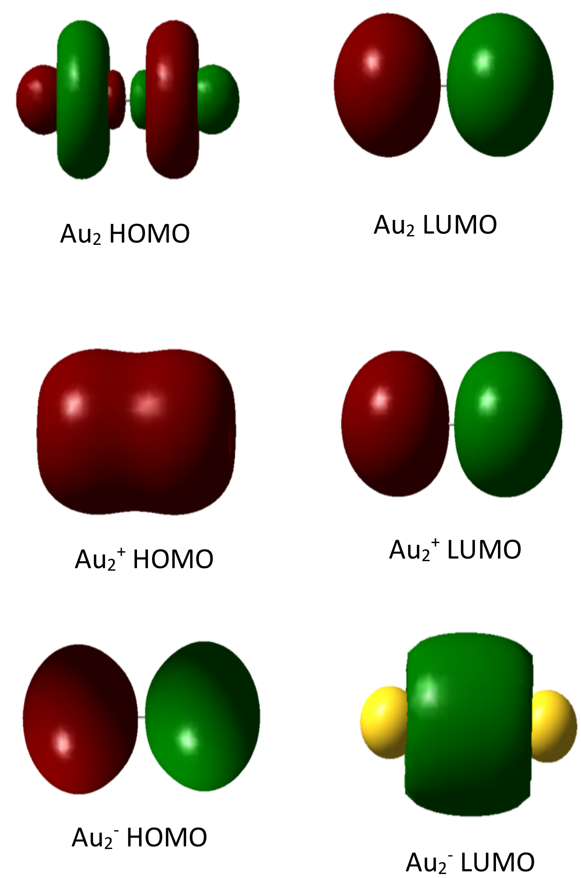

Fig. (1): The HOMO and LUMO contour maps.

Figure (2) displays the apparent changes in the contour diagrams of the surfaces of gold diatom following the addition or reduction of one electron. The addition or reduction of one electron causes a distortion in contour maps. The addition or reduction of single electron to the gold diatom weakens its decorative appearance, resulting in a less uniform structure compared to neutral Au_2 which has a smooth strong electrostatic potential.

Table 5: The vibration frequency and maximum wavelength of excitations and oscillator strength.

Model	Vib (cm^{-1})	λ_{max} (nm)	OS.
Au_2	171	447	0.1250
Au_2^+	137	1592 (exp. =1607)[15]	0.0012 (exp.=0.009) [15]
Au_2^-	131	562	0.1150

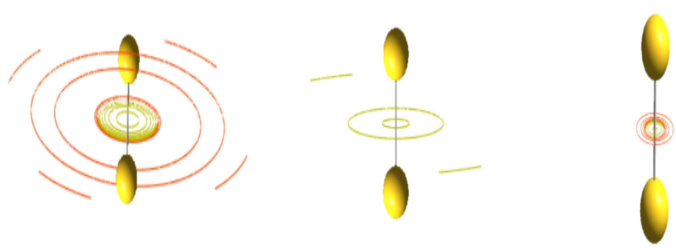

Fig. (2): The electrostatic potential contour maps.

Infrared spectroscopy may be used to study the frequencies of harmonic oscillations. The oscillations may be classified as either symmetric or asymmetric. Symmetric vibrations occur when atoms of the same kind oscillate, whereas asymmetric vibrations occur when atoms of different types oscillate. Infrared spectrum frequencies for the molecules Au_2, Au_2^+, and Au_2^- are generated using the Density Functional Theory (DFT) approach. Table 5 presented the vibration frequencies of Au_2, Au_2^+, and Au_2^-, where the neutral state of gold diatom has the strongest frequency. The single electron addition or reduction causes weakening the oscillation frequencies because of the distortion to the electronic charge over the whole gold diatom.

The electronic excitation spectra are investigated for Au_2, Au_2^+, and Au_2^-, that have been showed in figures 3-5. Table 5 presented maximum wavelength and oscillator strength of excitations. The neutral and anion states of gold diatom have the more probable UV/VIS absorption of light according to their oscillator strength, while the cation diatom has the weaker absorption and it shifted toward near-infrared. According to these results the optical response depends on the ionic state, where the photon absorption related with the electronic density of d diatom.

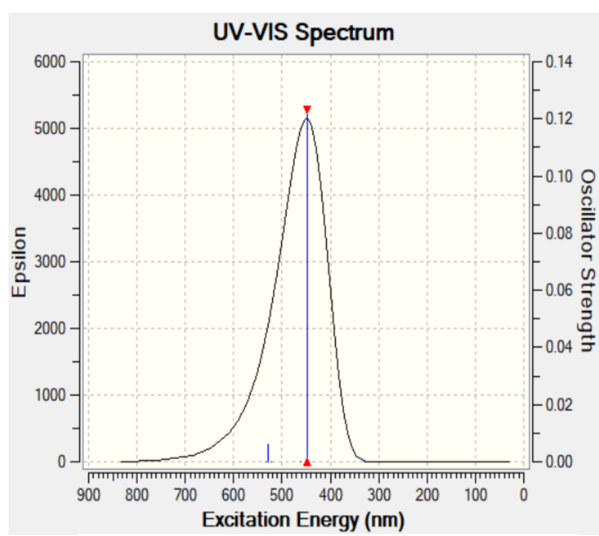

Fig. (3): The UV-VIS spectrum of Au_2 .

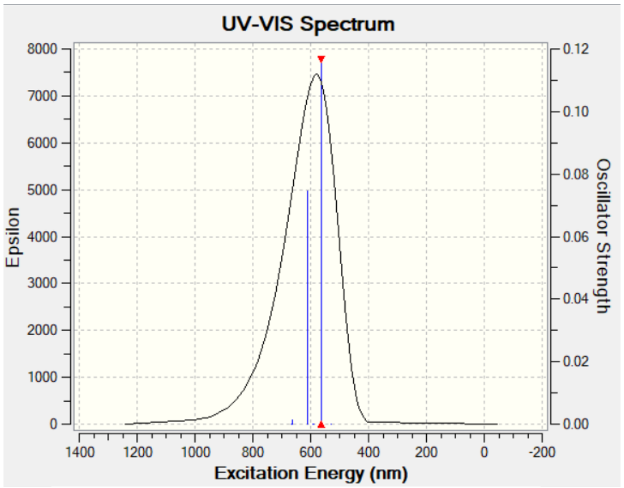

Fig. (5): The UV-VIS spectrum of Au_2^- .

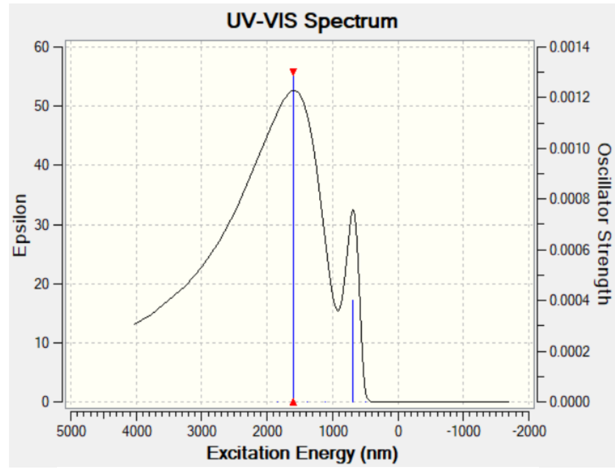

Fig. (4): The UV-VIS spectrum of Au_2^+ .

Within the scope of this work, the use of relativistic Density Functional Theory (DFT) with the Gaussian09 package is investigated for the purpose of analyzing the geometry optimization of gold diatoms in a variety of electronic states. The optimization is carried out at a number of different theoretical levels, such as B3LYP, cam-B3LYP, PBEPBE, HSE1PBE, and HSE2PBE, with the basis sets SDD and LaNL2MB being used. In order to investigate all of the structures, an inquiry has been carried out to examine their ionization potential, electron affinity, electrostatic potential contours, infrared spectra, molecular orbitals, energy gap, and electronic excitation. A high degree of concordance can be seen between the ionization potential and electron affinity of each and every structure and the experimental findings. The molecular orbitals of bonding and anti-bonding nature go through considerable alterations depending on the ionic state of the molecule. The electrostatic potential contours, vibration

4. Conclusion

frequency, and electronic excitation of a gold diatom are all determined by the electron charge density of the diatom. Hybrid functionals, which have a mixture of Hartree-Fock exchange with DFT exchange-correlation parts and the long range correction present good prediction of electronic properties for gold atom, diatom and ions. The relativistic basis set perform well to compute optical properties.

References

[1] Ren, X., Fu, J., Lin, X., Fu, X., Yan, J., Wu, R., Liu, J., and Huang, J., 2018, Cluster-to-cluster transformation among Au6, Au8 and Au11 nanoclusters, *Dalton Trans.*, 47, 7487-7491.

[2] Muñoz-Castro, A., 2022, On the ligand role in determining the compact or extended metallic core architecture in gold superatoms. Evaluation

of electronic and optical properties from relativistic DFT for [Au11(dppp)5]3+ and [Au11(dppe)6]3+ clusters, *Polyhedron*, 211, 1, 115572.

[3] He, S., Lv, Y., Wu, X., Zhao, Y., and Yu, H., 2022, Mechanistic insights into oxidation-induced size conversion of [Au6(dppp)4]2+ to [Au8(dppp)4Cl2]2+, *Inorg. Chem.*, 61, 49, 24.

[4] Häkkinen, H. and Landman, U., 2000, Gold clusters (AuN, 2<~N<~10) and their anions, *Phys. Rev. B*, 62, Issue 4-15, R2287.

[5] Grönbeck, H. and Andreoni, W., 2000, Gold and platinum microclusters and their anions: comparison of structural and electronic properties, *Chem. Phys.*, 262, Issue 1, pp. 1-14.

[6] Bravo-Pérez, G., Garzón, I. L., and Novaro, O., 1999, Ab initio study of small gold clusters, *J. Mol. Struct. THEOCHEM*, 493, 225-231.

[7] Kuang, X., Wang, X., and Liu, G., 2015, All-Electron Scalar Relativistic Calculations on the Adsorption of Small Gold Clusters Toward Methanol Molecule, *J. Nanosci. Nanotechnol.*, Vol. 15, No. 2, pp. 1269-1279.

[8] Wang, Y. and Zhou, G., 2022, DFT Investigations of Aun Nano-Clusters Supported on TiO2 Nanotubes: Structures and Electronic Properties, *Molecules*, 27, 2756.

[9] Wesendrup, R., Hunt, T., and Schwerdtfeger, P., 2000, Relativistic coupled cluster calculations for neutral and singly charged Au3 clusters, *J. Chem. Phys.*, 112, 21.

[10] Frisch, M. J., Trucks, G. W., Schlegel, H. B., et al., 2009, Gaussian 09, Revision A.02, *Gaussian, Inc.*, Pittsburgh PA.

[11] Reiher, M., 2006, Douglas–Kroll–Hess Theory: a relativistic electrons-only theory for chemistry, *Theor. Chem. Acc.*, 116, pp. 241–252.

[12] Hotop, H. and Lineberger, W. C., 1985, Binding Energies in Atomic Negative Ions: II, *J. Phys. Chem. Ref. Data*, 14, 731.

[13] Loock, H., Beaty, L. M., and Simard, B., 1999, Reassessment of the first ionization potentials of copper, silver, and gold, *Phys. Rev. A*, 59, 873.

[14] Suzumura, T., Nakajima, T., and Hirao, K., 1999, Ground-State Properties of MH, MCl, and M2 (M=Cu, Ag, and Au) Calculated by a Scalar Relativistic Density Functional Theory, *Int. J. Quantum Chem.*, Vol. 75, pp. 757-766.

[15] Dopfer, O., Förstel, M., Pollow, K., and Studemund, T., 2021, Near-infrared spectrum of the first excited state of Au2+, *Chem. Eur. J.*, 13.